Field Reversed Configuration Confinement Enhancement through Edge Biasing and Neutral Beam Injection

M. Tuszewski,[1] A. Smirnov,[1] M. C. Thompson,[1] S. Korepanov,[1] T. Akhmetov,[2] A. Ivanov,[2] R. Voskoboynikov,[2] L. Schmitz,[3] D. Barnes,[1] M. W. Binderbauer,[1] R. Brown,[1] D. Q. Bui,[1] R. Clary,[1] K. D. Conroy,[1] B. H. Deng,[1] S. A. Dettrick,[1] J. D. Douglass,[1] E. Garate,[1] F. J. Glass,[1] H. Gota,[1] H. Y. Guo,[1] D. Gupta,[1] S. Gupta,[1] J. S. Kinley,[1] K. Knapp,[1] A. Longman,[1] M. Hollins,[1] X. L. Li,[1] Y. Luo,[1] R. Mendoza,[1] Y. Mok,[1] A. Necas,[1] S. Primavera,[1] E. Ruskov,[1] J. H. Schroeder,[1] L. Sevier,[1] A. Sibley,[1] Y. Song,[1] X. Sun,[1] E. Trask,[1] A. D. Van Drie,[1] J. K. Walters,[1] and M. D. Wyman[1]

(The TAE Team)

[1]*Tri Alpha Energy, Inc., P.O. Box 7010, Rancho Santa Margarita, California 92688, USA*
[2]*Budker Institute of Nuclear Physics, Novosibirsk, 630090, Russia*
[3]*Department of Physics and Astronomy, UCLA, Los Angeles, California 90095-1547, USA*
(Received 17 April 2012; published 21 June 2012)

Field reversed configurations (FRCs) with high confinement are obtained in the C-2 device by combining plasma gun edge biasing and neutral beam injection. The plasma gun creates an inward radial electric field that counters the usual FRC spin-up. The $n = 2$ rotational instability is stabilized without applying quadrupole magnetic fields. The FRCs are nearly axisymmetric, which enables fast ion confinement. The plasma gun also produces $E \times B$ shear in the FRC edge layer, which may explain the observed improved particle transport. The FRC confinement times are improved by factors 2 to 4, and the plasma lifetimes are extended from 1 to up to 4 ms.

DOI: 10.1103/PhysRevLett.108.255008 PACS numbers: 52.55.−s

The field reversed configuration (FRC) is a prolate compact toroid formed with poloidal magnetic fields [1,2]. There is continued interest in FRC research because it offers a high potential for a fusion reactor, including very high-beta, simple geometry, natural divertor, and ease of translation. The FRC could lead to an economic fusion reactor with high fusion power density, possibly using aneutronic fuels.

Large FRC equilibria are produced in the C-2 device by combining dynamic formation and merging processes [3,4]. An example is shown in Fig. 1, as calculated from the Lamy-Ridge code [5]. Field line contours are traced, and plasma densities are indicated with colors. Typical equilibrium FRC parameters at $t = 0.3$ ms (FRC formation starts at $t = 0$) are: separatrix radius $r_s \sim 0.4$ m, separatrix length $L_s \sim 3$ m, edge magnetic field $B_e \sim 1$ kG, average density $\sim 4 \times 10^{19}$ m^{-3}, deuterium ion temperature ~ 0.5 keV, and electron temperature ~ 0.2 keV.

The main goal of the C-2 experiment is to demonstrate FRC sustainment with Neutral Beam (NB) injection for heating and current drive, and with pellet injection for particle refueling. The C-2 NBs (20 keV Hydrogen, ~ 4 MW) are injected tangentially to the FRC current (coinjection) with an impact parameter of 0.2 m. This permits current drive, in a way similar to past 2XIIB experiments [6], but with a field reversed plasma target. Past C-2 FRCs [3,4] had relatively good confinement properties, but global power losses (~ 10 MW) exceeded the available NB input power. Hence, the FRC confinement must be further improved.

Rotational instabilities [3,4] are also a concern for NB fast ions because they break the FRC azimuthal symmetry. Multipole magnetic field stabilization [7] of rotational modes is effective, but it also breaks azimuthal symmetry and can cause rapid stochastic diffusion of the NB fast ion orbits [8,9]. Similar fast ion losses are calculated for FRCs sustained with rotating magnetic fields [10]. A new axisymmetric technique to control FRC rotational instabilities is therefore highly desirable.

A plasma gun, recently added to the C-2 device, proves successful in (i) controlling FRC rotational instabilities while preserving axisymmetry, hence enabling NB fast ion confinement, and (ii) creating $E \times B$ velocity shear just outside of the separatrix, possibly yielding improved FRC confinement. In this Letter, we report these encouraging results achieved with the first stabilized FRCs held in axisymmetric fields. These new edge biasing experiments also stand as fundamental physics since the FRC geometry is very simple.

The plasma gun is located in the C-2 South divertor ($z = -8$ m) as sketched in Fig. 1. Two magnetic end plugs (0.25 m diameter, <2 T) at $z = \pm 7.3$ m help to reduce gas leakage from the gun to the main chamber. The plasma gun, used previously on the AMBAL tandem mirror device [11,12], is sketched in Fig. 2. An annular (0.11 m inner diameter, 0.13 m outer diameter) plasma stream ($\sim 10^{22}$ D/s for 6 ms) is created with two gas valves and an arc discharge (~ 10 kA). The gun includes a (< 0.5 T) pulsed magnet. The gun produces a hot ($T_e \sim 30$–50 eV,

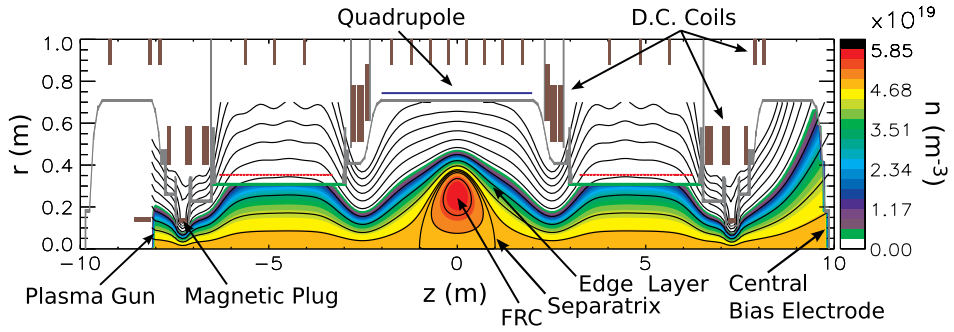

FIG. 1 (color online). Sketch of an FRC equilibrium inside the modified C-2 device.

$T_i \sim 100$ eV) tenuous ($< 10^{19}$ m^{-3}) plasma stream after FRC formation, as measured in front of the gun with diamagnetic loops, Langmuir probes, and microwave interferometry.

The gun creates an inward electric field in the plasma stream, and the electric potential follows approximately magnetic field lines. The gun anode to cathode voltage drop is typically ~500 V. The plasma gun floating electrode (Fig. 2) measures ~ -450 V and the anode voltage is ~50 V. Floating potentials of the gun plasma alone, measured with a triple probe 1 m in front of the gun ($z = -7$ m), are shown in Fig. 3(a). The floating potentials have a minimum value on axis similar to the gun floating electrode potential. The radial profiles in Fig. 3(a), and others obtained at $z = 0$, show that the floating potentials follow field line contours. The North divertor central bias electrode ($z = 10$ m, see Fig. 1) tracks the gun floating electrode at all times, indicating a good electrical connection through the 18 m device length.

The plasma floating potentials in the FRC edge layer are shown in Fig. 3(b), with and without the plasma gun activated. These triple probe data, obtained at $z = 0$ and at $t = 0.3$ ms, are averaged over several similar FRC discharges. Typical standard deviations are indicated. With the plasma gun off, the floating potentials decrease monotonically with radius. With the plasma gun on, the floating potentials increase with radius in the edge layer (first 5 to 10 cm outside the separatrix), suggesting an inward radial electric field. These trends are only qualitative because floating rather than plasma potentials are shown in Fig. 3. Probe measurements become increasingly difficult close to the FRC separatrix, and no data are available for $r < 0.4$ m.

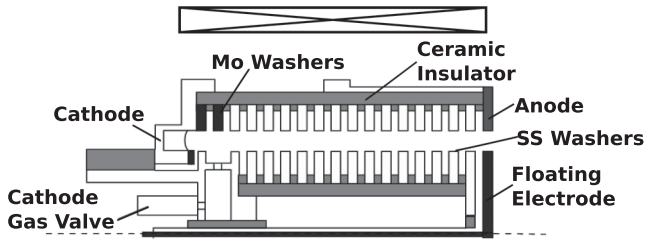

FIG. 2. Cross-sectional schematic of the AMBAL plasma gun.

The plasma gun inward electric field counters the usual FRC spin-up. The FRC ion velocity can be expressed from the momentum equation as

$$\mathbf{v}_i = \mathbf{v}_{Di} + \mathbf{v}_{E\times B} = (\mathbf{B} \times \nabla_{pi})/(neB^2) + (\mathbf{E} \times \mathbf{B})/B^2 \quad (1)$$

The ion velocity is the sum of the diamagnetic velocity $\mathbf{v}_{Di}$ and of the $\mathbf{E} \times \mathbf{B}$ velocity $\mathbf{v}_{E\times B}$. At the FRC midplane, $\mathbf{B}$ is axial, $\mathbf{E}$ and ∇p_i are radial, and $\mathbf{v}_i$ is azimuthal (cylindrical coordinates). With the plasma gun off, $\mathbf{E}$ is outward and opposes ∇p_i, so that $\mathbf{v}_{E\times B}$ adds to $\mathbf{v}_{Di}$. Hence,

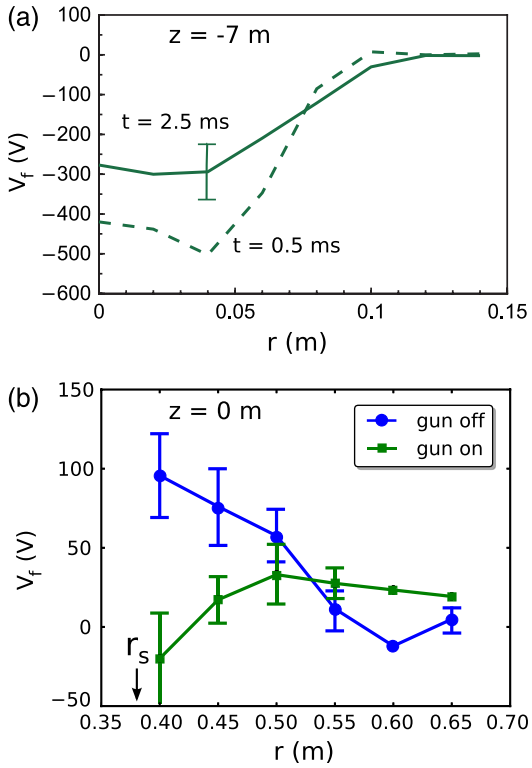

FIG. 3 (color online). Radial profiles of probe floating potentials (a) at $z = -7$ m with plasma gun on and no FRC, and (b) at $z = 0$ with plasma gun on and off.

the rotational parameter $\alpha = v_i/v_{Di}$ exceeds unity, and the dangerous $n = 2$ mode can grow [1]. With the plasma gun on, both $\mathbf{E}$ and ∇p_i are inward near the FRC separatrix, $\mathbf{v}_{E\times B}$ opposes $\mathbf{v}_{Di}$, and the $n = 2$ rotational mode cannot grow ($\alpha < 1$).

FRC discharges operated with the plasma gun on and off are compared in Fig. 4. Line-integrated densities from CO_2 side-on interferometry [13] at $z = 0$ are shown as functions of time. No quadrupole magnetic fields are applied. The discharge with plasma gun off shows large $n = 2$ mode oscillations [14] between 0.3 and 0.8 ms. Mirnov probe arrays also reveal some $n = 1$ rotational wobble [1,15] through the discharge, with a slow rotation primarily in the ion diamagnetic direction. The discharge with plasma gun on does not show $n = 2$ oscillations, but some $n = 1$ wobble is apparent between 1.5 and 2 ms. This $n = 1$ mode rotates in the electron diamagnetic direction, and its amplitude is relatively small, which could indicate partial line-tying [16] to the gun anode.

The plasma gun stabilizes the lowest-order FRC rotational instabilities without using external multipoles. Higher-order rotational modes are not observed, consistent with finite Larmor radius stabilization [17]. Hence, the gun-assisted FRC discharges are nearly axisymmetric. As a result, the NB fast ion confinement is significantly improved and the discharges show much improved stability and confinement properties.

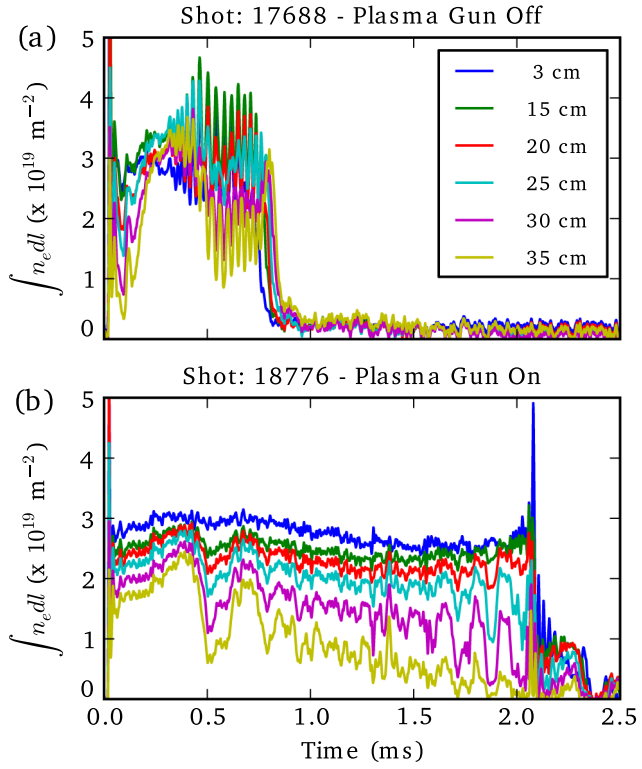

FIG. 4 (color online). Line-integrated densities of 2 C-2 FRC discharges with (a) plasma gun off, and (b) plasma gun on.

The plasma gun provides significant $E \times B$ velocity shear in the FRC edge layer. The $E \times B$ velocities (and the E_r values) of C-2 discharges are estimated, for the first time in an FRC experiment, with multichannel Doppler backscattering. Such measurements [18,19] utilize six collinear Gaussian diagnostic microwave beams (spot size ~4.5 cm at 45 GHz) launched at $z = 0.5$ m on the C-2 device. The probed wave number k_θ is obtained using ray tracing based on the FRC density radial profiles. The instantaneous Doppler shift, $f_D = (\omega_R - \omega_I)/2\pi$, permits one to estimate $\mathbf{v}_{E\times B} \sim 2\pi f_D/k_\theta$ and to extract $E_r = \mathbf{v}_{E\times B}B_z$ assuming a rigid rotor profile [1] ($B_z = B_e \tanh[K(2r^2/r_s^2 - 1)]$ with $K \sim 1.2r_s/r_w$).

The reflectometer E_r radial profiles in the FRC edge layer are shown in Fig. 5 at various times, for a discharge with the plasma gun on. One observes $E_r < 0$ a few cm outside the FRC separatrix, and $E_r > 0$ for larger radii, in qualitative agreement with the gun on probe data in Fig. 3(b). The $E_r < 0$ radial extent is consistent with the plasma gun stream flowing along field lines. The minimum reflectometer value, $E_r \sim -1$ kV/m, is also consistent with that (~ -0.8 kV/m) estimated from differentiating between 0.4 and 0.45 m the probe data in Fig. 3(b). Similar edge E_r reversal has been measured with ion spectroscopy in the RFX reversed field pinch device [20].

The $E \times B$ velocity shear is determined mostly by E_r since B_z increases slowly with radius in the edge layer. The $E \times B$ shearing rate can be estimated from the reflectometer data as $\omega_{E\times B} = d/dr(\mathbf{v}_{E\times B})$ near the FRC midplane. One obtains $\mathbf{v}_{E\times B} \sim 10$ km/s and $\omega_{E\times B} \sim 10^5$ rad/s near the separatrix. These values are comparable in magnitude to those observed in other magnetically confined fusion plasmas [20,21]. The shearing rates are comparable to the linear growth rates ($\sim 2v_A/L_s$) of several FRC instabilities predicted near the FRC separatrix, such as interchanges and co-interchanges [1]. Hence, $E \times B$ velocity shear may well reduce turbulent particle transport in C-2 discharges with plasma gun on. Reflectometer data, to be detailed elsewhere, suggest reduced density fluctuation levels with the plasma gun on.

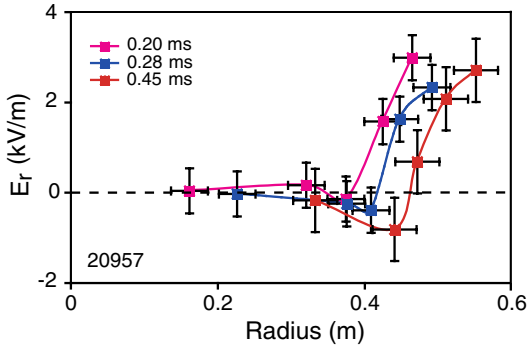

FIG. 5 (color online). Electric field radial profiles from reflectometer Doppler backscattering data. The profiles are shown at selected times for an FRC discharge with the plasma gun on.

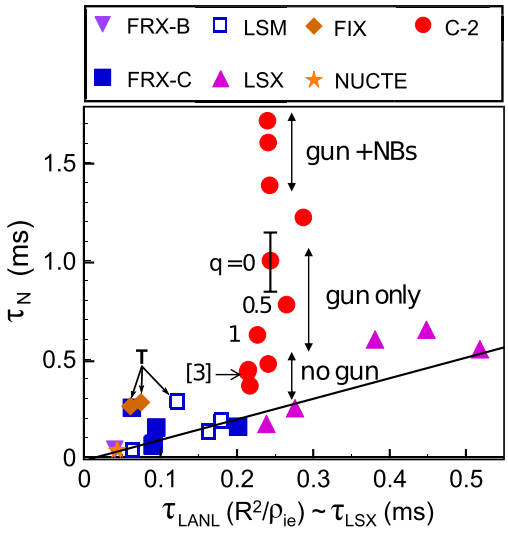

FIG. 6 (color online). FRC particle confinement times in the C-2 device and in other FRC experiments.

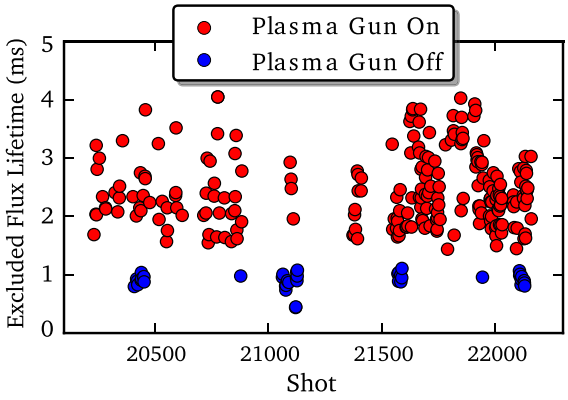

FIG. 7 (color online). Plasma lifetimes for C-2 discharges with plasma gun on and off.

Selected FRC particle confinement times τ_N are compared in Fig. 6 against empirical FRC scaling laws [22,23]. FRC particle confinement was shown to scale approximately as R^2/ρ_{ie} ($R = r_s/\sqrt{2}$ and ρ_{ie} is the ion gyroradius evaluated with the edge magnetic field B_e) from data obtained in the Los Alamos National Laboratory (LANL) FRX-B and FRX-C devices [22], and from subsequent FRX-C/LSM (LSM) data. This empirical scaling law, τ_{LANL}, is indicated with a solid line in Fig. 6. Later data from the Large s Experiment (LSX) [23] confirmed approximately this empirical scaling law, as shown in Fig. 6.

The values of τ_N in Fig. 6 are $1/e$ decay times of the FRC separatrix particle inventory, estimated from combined excluded flux and side-on interferometry data over the first half millisecond. All τ_N values are averaged over many similar FRC discharges. Some translated FRC data (indicated with a T and arrows in Fig. 6) show improved particle confinement by about a factor of 2 compared to the empirical scaling law. The particle confinement times of translated C-2 FRCs without the plasma gun also show similar factor of 2 improvement. One of those C-2 points (labeled [3] in Fig. 6) comes from a recently published data set [3]. Most C-2 data have $r_s \sim 40$ cm and $\rho_{ie} \sim 3$ cm; hence, $R^2/\rho_{ie} \sim 250$ μs (times in μs with dimensions in cm).

A significant increase in the C-2 FRC particle confinement is observed in Fig. 6 with the plasma gun only (no NB injection), and with no quadrupole magnetic fields ($q = 0$). The normalized quadrupole strength $q = 1$ (15 kA in each quadrupole bar) is sufficient for $n = 2$ stabilization [4]. The FRC particle confinement degrades as q increases because the magnetic fields fan in and out, as in some mirror machines [24]. The edge layer field lines reach the wall near the ends of the C-2 confinement vessel for $q \sim 0.5$, compromising the connection to the plasma gun. The FRC particle confinement further improves with NB injection. The best C-2 data have $\tau_N \sim 1.7$ ms, a factor of 4 above C-2 data without the plasma gun [3,4], and a factor of 7 above the scaling laws. Clearly, these empirical yard sticks are no longer relevant.

All FRC confinement times (magnetic flux, particle, and energy) appear to improve with the plasma gun and with NB injection. However, the magnetic flux and energy confinement times are affected by the NB fast ion population. Particle confinement times are more reliable because NB injection (< 250 A) is a negligible particle source. Measurements and calculations indicate that the gun plasma stream and neutral gas ionization are also small particle sources inside the FRC separatrix. Hence, the FRC particle inventory is not sustained in present experiments, and it decays roughly exponentially on a time scale τ_N (Fig. 6).

Many aspects of the data presented in this Letter require clarification with additional experimental and theoretical research. Plasma gun operation with higher charging voltages, and operation with two plasma guns are being considered to further increase the $E \times B$ velocity shear in the edge layer. Long-lived FRCs could not be obtained without NB injection. The respective contributions of the plasma gun and of the NBs are currently under detailed investigation. The combined effects of the plasma gun and of NB injection permit us to extend the plasma (diamagnetism) lifetimes from about 1 to 4 ms, as shown in Fig. 7. For the best FRC discharges with plasma gun and NBs on, the FRC global power losses are $\sim$4 MW at $t \sim 1$ ms (plasma energy $\sim$2 kJ, global energy confinement time $\sim$0.5 ms), which is within reach of the available injected NB power.

In summary, a plasma gun, placed at one end of the C-2 device, yields an inward radial electric field in the FRC edge layer. This counters the usual FRC spin-up and permits us to control the dangerous $n = 2$ rotational instability without applying quadrupole magnetic fields. The FRC discharges are nearly axisymmetric, which improves NB fast ion confinement. The plasma gun also creates $E \times B$

velocity shear in the FRC edge layer, which may explain the improved FRC particle confinement. The FRC particle confinement times are improved by factors 2 to 4 compared to previous C-2 data without the plasma gun, and by factors up to 7 compared to past empirical scaling laws. The combined effects of the plasma gun and of NB injection yield plasma lifetimes up to 4 ms, and permit future attempts at FRC sustainment.

We thank our shareholders for their support and trust, and the rest of the TAE staff for their dedicated, excellent work. We are especially thankful to many members of the Budker Institute for providing the plasma gun and the neutral beams.

[1] M. Tuszewski, Nucl. Fusion **28**, 2033 (1988).
[2] L. C. Steinhauer, Phys. Plasmas **18**, 070501 (2011).
[3] M. Binderbauer, H. Y. Guo, M. Tuszewski, S. Putvinski, L. Sevier, D. Barnes, N. Rostoker, M. G. Anderson, R. Andow *et al.*, Phys. Rev. Lett. **105**, 045003 (2010).
[4] H. Y. Guo, M. W. Binderbauer, D. Barnes, S. Putvinski, N. Rostoker, L. Sevier, M. Tuszewski, M. G. Anderson, R. Andow *et al.*, Phys. Plasmas **18**, 056110 (2011).
[5] L. Galeotti, D. C. Barnes, F. Ceccherini, and F. Pegoraro, Phys. Plasmas **18**, 082509 (2011).
[6] W. C. Turner, J. F. Clauser, F. H. Coensgen, D. L. Correll, W. F. Cummins, R. P. Freis, R. K. Goodman, A. L. Hunt, T. B. Kaiser, G. M. Melin, W. E. Nexsen, T. C. Simonen, and B. W. Stallard, Nucl. Fusion **19**, 1011 (1979).
[7] S. Ohi, T. Minato, Y. Kawakami, M. Tanjyo, S. Okada, Y. Ito, M. Kako, S. Goto, T. Ishimura, and H. Iton, Phys. Rev. Lett. **51**, 1042 (1983).
[8] J. M. Finn, Plasma Phys. **21**, 405 (1979).
[9] R. H. Cohen, D. V. Anderson, and C. B. Sharp, Phys. Rev. Lett. **41**, 1304 (1978).
[10] A. F. Lifschitz, R. Farengo, and A. L. Hoffman, Nucl. Fusion **44**, 1015 (2004).
[11] G. I. Dimov, A. A. Ivanov, and G. V. Roslyakov, Sov. J. Plasma Phys. **8**, 546 (1982).
[12] T. D. Akhmetov, V. S. Belkin, I. O. Bespamyatnov, V. I. Davydenko, G. I. Dimov, Yu. V. Kovalenko, A. S. Krivenko, P. A. Potashov, V. V. Razorenov, V. B. Reva *et al.*, Trans. Fusion Sci. Technology **43**, 58 (2003).
[13] O. Gornostaeva, B. H. Deng, E. Garate, H. Gota, J. Kinley, J. Schroeder, and M. Tuszewski, Rev. Sci. Instrum. **81**, 10D516 (2010).
[14] M. Tuszewski, Plasma Phys. Controlled Fusion **26**, 991 (1984).
[15] M. Tuszewski, G. A. Barnes, M. H. Baron, R. E. Chrien, W. N. Hugrass, P. L. Klingner, Chun Ng, D. J. Rej, D. P. Taggart, R. E. Siemon, and B. L. Wright, Phys. Fluids B **2**, 2541 (1990).
[16] A. W. Molvik, R. A. Breun, S. N. Golovato, N. Hershkowitz, B. McVey, R. S. Post, D. Smatlak, and L. Yujiri, Phys. Fluids **27**, 2711 (1984); D. Ryutov, H. L. Berk, B. I. Cohen, A. W. Molvik, and T. C. Simonen, Phys. Plasmas **18**, 092301 (2011).
[17] M. N. Rosenbluth, N. A. Krall, and N. Rostoker, Nucl. Fusion Suppl., **1**, 143 (1962).
[18] M. Hirsch, E. Holzhauer, J. Baldzuhn, B. Kurzan, and B. Scott, Plasma Phys. Controlled Fusion **43**, 1641 (2001).
[19] L. Schmitz, G. Wang, J. C. Hillesheim, T. L. Rhodes, W. A. Peebles, A. E. White, L. Zeng, T. A. Carter, and W. Solomon, Rev. Sci. Instrum. **79**, 10F113 (2008).
[20] L. Carraro, M. E. Puiatti, F. Sattin, P. Scarin, and M. Valisa, Plasma Phys. Controlled Fusion **40**, 1021 (1998).
[21] K. H. Burrell, Phys. Plasmas **4**, 1499 (1997).
[22] K. F. McKenna, W. T. Armstrong, R. R. Bartsch, R. E. Chrien, J. C. Cochrane, Jr., R. W. Kewish, Jr., P. Klingner, R. K. Linford, D. J. Rej, E. G. Sherwood, R. E. Siemon, and M. Tuszewski, Phys. Rev. Lett. **50**, 1787 (1983).
[23] A. L. Hoffman and J. T. Slough, Nucl. Fusion **33**, 27 (1993).
[24] R. F. Post, Nucl. Fusion **27**, 1577 (1987).